ВЫСОКОМОЛЕКУЛЯРНЫЕ СОЕДИНЕНИЯ, Серия А, 2011, том 53, № 1, с. 27–31

УДК 541(64+13):543.42

ELECTROCHEMICAL SYNTHESIS OF POLY(*O*-TOLIDINE): ELECTROCHEMICAL AND SPECTROSCOPIC CHARACTERIZATION[1]

© 2011 г. M. Guergouri and L. Bencharif

Laboratoire de Chimie Des Matériaux, Département de Chimie, Faculté des Science, Université Mentouri-Constantine-25000, Algérie

e-mail: cmaya79@yahoo.fr

Received December 13, 2009;
Revised Manuscript Received February 18, 2010

Abstract—Polymerization of (*O*-tolidine), as ring substituted derivative of benzidine was achieved electrochemically in organic solution containing Bu_4NBF_4 (0.2 M) in dichloromethane as supporting electrolyte. The film was obtained by electropolymerization in solution containing monomer in various ratio ((5×10^{-4})–(5×10^{-2}) M). This polymer was characterized by cycling voltammetry, impedance measurement, UV-visible and FT-IR spectroscopy.

INTRODUCTION

In the last twenty years, a great scientific attention has been paid to electroconductive polymers such as poly(acetylene)s, poly(thiophene)s, poly(pyrrole)s, poly(aniline)s, etc. Polyaniline (PANI) is one of the most intensively investigated conductive organic polymers because of its interesting properties, e.g., high levels of doping [1], catalytic activities [2], electrochromic nature [3], electrochemical redox behaviour [4] and due to its possible use in technological commercial applications [5] such as rechargeable batteries, catalysis, corrosion protection, antistatic materials, textile industry.

PANI can be easily prepared by several techniques including chemically oxidative polymerization [6, 7] electrochemically oxidative polymerization [8, 9], plasma polymerization [10] and photoinduced electron-transfer photooxidative polymerization [11]. The proprieties and applications of PANI were reviewed in detail by Genies and al. [12].

The success of PANI has attached many investigators to study the synthesis and properties of the polymers from aromatic diamines. Theses monomers are very susceptible to oxidative polymerization via oxidation of one or both amino groups to give linear polymer [13]. Thus, Arsov and co-workers [14] have shown that poly(2-methyl aniline) can be synthesized electrochemically in various concentrations of acidic medium. In the same way, electroactive polybenzidine can be prepared by electrochemical oxidation of benzidine in aqueous solution [15] and by thermal method [16].

The electrochemical oxidation of polynuclear amine in non-aqueous medium has been much less studied. In this article, we report the electrochemical synthesis of poly(*O*-tolidine) and its characterization using in particular cyclic voltammetry, UV-visible and infrared spectroscopy.

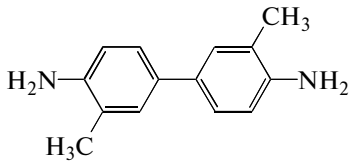

3,3'-dimethyl-1,1'-biphenyl-4,4'-diamine (*O*-tolidine)

EXPERIMENTAL METHODS

Electrochemical measurements

Prior to the electrochemical polymerization, *O*-tolidine was purified by recrystallization in ethanol. Tetrabutylammonium tetrafluoroborate was recrystallized in a mixture of water/methanol and dried at 100°C for 24 h; aluminium oxide was dried at 300°C under vacuum for at least 24 h prior to use. Dichloromethane was dried by refluxing over calcium chloride prior to use.

Table 1. Redox potentials and current densities of *O*-tolidine

Concentration of monomer, M	Redox potential, mV		Current density, μA/cm^2	
	1st peak	2nd peak	1st peak	2nd peak
5×10^{-2}	203	786	90.23	131.30
10^{-2}	113	666	22.04	40.65
5×10^{-3}	98	650	15.51	27.61
10^{-3}	124	628	6.12	10.8
5×10^{-4}	135	618	4.49	8.73

[1] Статья печатается в представленном авторами виде.

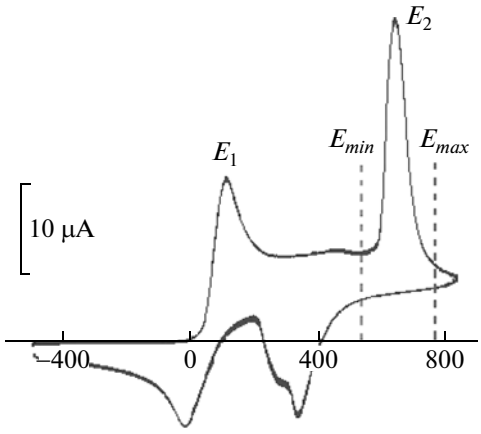

Fig. 1. Cyclic voltammogram in dry CH_2Cl_2 + 0.2 M Bu_4NBF_4 (containing Al_2O_3) of *O*-tolidine 5×10^{-3} M, scanning between –0.5 and 0.8 V. Scan rate: 100 mV s^{-1}. $E_{min} - E_{max}$: potential plage of electropolymerization.

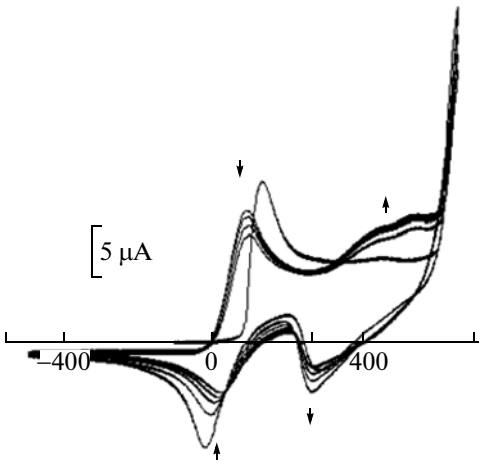

Fig. 2. Cyclic voltammogram in dry CH_2Cl_2 + 0.2 M Bu_4NBF_4 (containing Al_2O_3) of *O*-tolidine 5×10^{-3} M, scanning between –0.5 and 0.65 V. Scan rate: 100 mV s^{-1}. Five cycles.

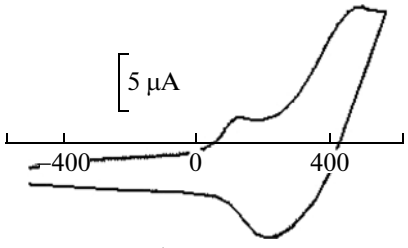

Fig. 3. Cyclic voltammogram in dry CH_2Cl_2 + 0.2 M Bu_4NBF_4 (containing Al_2O_3) of a film prepared previously at 0.65 V in dry CH_2Cl_2 + 0.2 M Bu_4NBF_4 with 5×10^{-3} M of *O*-tolidine. Scan rate: 100 mV s^{-1}.

Electrochemical experiments were performed using a Pt disk electrode (diameter 1mm), a Pt wire in a 0.1 M $AgNO_3/CH_3CN$ as reference electrode. Activated Al_2O_3 was added into the electrolytic solution to remove excess moisture. The electrochemical cell used was of the three-electrode type with separate compartments for the reference electrode and the counter-electrode. It was connected to a PGZ301 Potentiostat, interfaced to a PC.

All data were collected and analyzed using Voltamaster software. All solutions were deaerated by bubbling argon gas for a few minutes prior to electrochemical measurements.

Spectroscopic measurements

IR spectra were recorded ex-situ using spectrophotometer FTIR-8201PC SHIMADZU by diffuse reflectance through the polymer mixed with KBr. The optical absorption study of the product was carried out using UV-Visible spectrophotometer (Heλiosα). The UV-Visible spectra were obtained ex-situ in DMF. All the spectra were recorded in the wavelength range 200–600 nm.

RESULTS AND DISCUSSION

Anodic oxidation of O-tolidine

Anodic oxidation of *O*-tolidine was carried by cyclic voltammetry. The potential of the working electrode is scanned between –0.5 and 0.8 V at 100 mV/s in solution containing *O*-tolidine at different ratio of concentration ((5×10^{-4})–(5×10^{-2}) M) in CH_2Cl_2/Bu_4NBF_4 (0.2 M).The redox potentials and current densities of the two observed peaks are summarized in Table 1.

The lower potential corresponding to the first anodic peak is observed with 5×10^{-3} M of *O*-tolidine. There is no regular relationship between the oxidation potential value and measuring conditions [13], this indicating that the first oxidation potential is an easily variable and instable parameter; on the contrary, the current intensities increase normally with the concentration of monomer. The best and defined overall voltammogram is obtained with 5×10^{-3} M of *O*-tolidine (Fig. 1).

Electrodeposition was performed by cycle potential sweeping in the potential range between –0.5 and 0.65 V, versus Ag/Ag^+ 0.1 M in CH_3CN at a scan rate of 100 mV s^{-1} (Fig. 2) in non-aqueous solution using Bu_4NBF_4 (0.2 M) in dichloromethane as supporting electrolyte.

The oxidation occurs in two steps: a first wave E1 at 0.098 V followed by a second one E2 at 0.65 V. The first wave E1 shifts at less anodic potentials after the first scan and is associated at the formation of radical-cation ($M^{\cdot+}$) which, after a rapid coupling with another

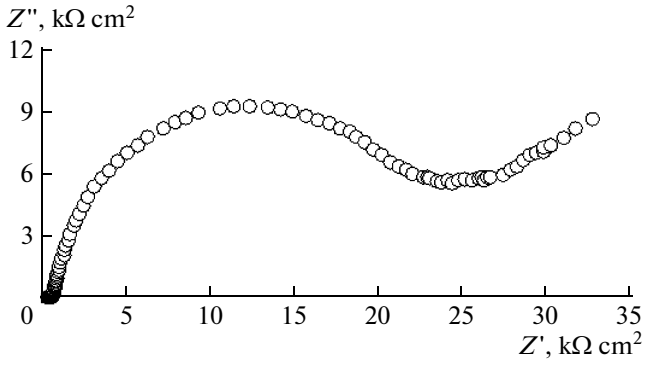

Fig. 4. Nyquist plot for Pt/poly(*O*-tolidine) at 0.55 V (vs. Ag/Ag^+ 0.1 M in CH_3CN) in a 0.2 mol/l of Bu_4NBF_4/ CH_2Cl_2.

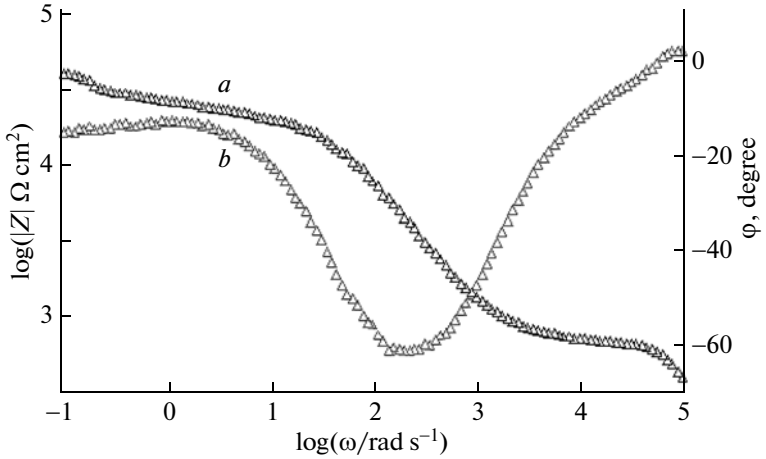

Fig. 5. (a) log*Z*–logω plot, (b) phase angle–logω plot for Pt/poly(*O*-tolidine) at 0.55 V (vs. Ag/Ag^+ 0.1 M in CH_3CN) in a 0.2 mol/l of Bu_4NBF_4/ CH_2Cl_2.

radical-cation and deprotonation gives the dimer (D). The dependence of the first peak potentials on the logarithm of the scan rate at moderate to relatively high scan rates indicates that the disappearance of the electrogenerated species corresponds to the coupling of two cation radicals [17]. The second wave E2 would correspond to the oxidation of the dimmer.

$$M \xrightarrow{-e^-} M^{\bullet +}$$

$$2M^{\bullet +} \xrightarrow{-2H^+} D$$

$$D \xrightarrow{-e^-} D^{\bullet +}$$

$$2D^{\bullet +} \longrightarrow \text{polymer}$$

Scanning potentials between –0.5 V and 0.65 V shows a regular decrease in response of the first wave and a growth of a new redox system between 0.2 V and 0.6 V. Otherwise when scanning is performed up to 0.8 V, a dark thick deposit film is observed and the return voltammetric response is poor. In the next scans, the waves have strongly decreased and this is explained by the formatting of non-conductive film in this potential range.

Polymerization occurs also during fixed potential oxidations (E = 0.65 V). The resulting blue-black coated platinum electrode is thoroughly rinsed with water and cycled between –0.5 et 0.53 V in electroactive solution free of monomer until a steady cyclic voltammogram is obtained. The film has a redox potential of +0.48 V as showing in Fig. 3.

Electrochemical impedance spectroscopy

This technique can be used to check whether electrode surface is modified or not. All data were obtained for poly(*O*-tolidine)-coated platinum electrode at fre-

Table 2. Ohmic resistance, charge transfer resistance and capacity data for Pt/poly(*O*-tolidine) obtained from electrochemical impedance spectroscopy measurements at 0.55 V (vs. Ag/Ag^+ 0.1 M in CH_3CN) in a 0.2 mol/L of Bu_4NBF_4/CH_2Cl_2 with 5×10^{-3} M of *O*-tolidine

Double-layer capacity C_{dl}	Charge transfer resistance R_{ct}	Ohmic resistance of the cell R_e
3.25 mF/cm^2	22.86 kΩ cm^2	743.2 Ω cm^2

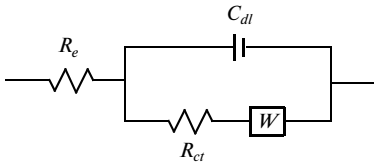

Fig. 6. Equivalent circuit with mixed kinetic and charge transfer control.

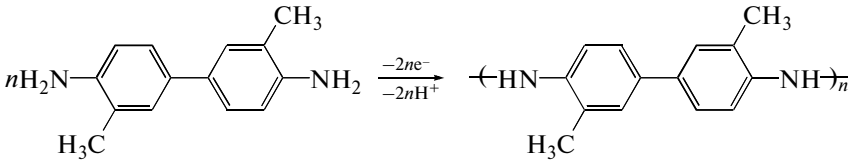

Fig. 7. Formation of poly(*O*-tolidine).

quency varying from 0.1 Hz to 100 kHz in CH_2Cl_2 solution containing 0.2 M Bu_4NBF_4, at potential corresponding to the range of p-doping processes (example: $E = 0.55$ V). For a modified electrode, the Nyquist plot (imaginary impedance Z'' vs. real impedance Z') shows three characteristic parts of the spectra: semicircle with Z' axis intercept in the higher frequency range (R_e) due to charge transfer, a short transition region that looks like the Warburg one due to diffusion impedance at the electrode-electrolyte interface and a straight line at low frequencies [18, 19].

The values of the ohmic resistance (R_e) and the charge transfer resistance (R_{ct}) are obtained by the intercept of the curve with the real axis at the higher-frequency and lower-frequency area respectively Fig. 4.

Table 3. FTIR spectroscopy data of *O*-tolidine and poly(*O*-tolidine)

Assignments for IR absorption bands cm^{-1}		Vibrations
O-tolidine	poly(*O*-tolidine)	
734–883	663–820	C–H out-of-plane deformation
–	919–1105	BF_4^- doping species
1379	1371–1397	CH_3 group symmetric deformation
1452–1491	1521	C=C stretching
–	1568	NH–NH deformation
1624	1624	N–H
2933	2871–2960	Aromatic C–H stretching
3014–3747	3246–3851	Alkyl C–H stretching
3337–3468	–	N–H stretching
–	3377	Single N–H stretching

Capacity value (C_{dl}) is calculated from the relation [20]:

$$C_{dl} = 1/(2\pi f Z')$$

Both plots (log|*Z*| and phase angle φ vs. logω) of poly(*O*-tolidine) films are shown in Fig. 5.

The equivalent circuit (Fig. 6) corresponds to an electrode with a double-layer capacity C_{dl} and simultaneous electrode reaction with charge transfer resistance R_{ct}.

The circuit models a cell where polarization is due to a combination of kinetic and diffusion processes. A measured data are summarized in Table 2.

Infra-red spectroscopy

The FT-IR spectroscopy of *O*-tolidine and poly(*O*-tolidine) is performed in a KBr mixed powder. The IR band positions of the poly(*O*-tolidine) are shown in Table 3.

The most of monomer bands have been conserved in the polymer spectrum. However, a band at 3336.6–3467.8 cm^{-1} on the monomer spectrum ascribed to the NH_2 elongation nearly disappears and is replaced by a band at 3377 cm^{-1} attributed to the N–H stretching of the polymer structure. This fact suggests that the NH_2 groups take part in the electropolymerization (Fig. 7). Furthermore, on the p-doped poly(*O*-tolidine), the band at 1031cm^{-1} is associated to the BF_4^- doping species vibration.

UV-visible spectroscopy

Figure 8 shows UV-visible spectra of *O*-tolidine and p-doped poly(*O*-tolidine) recorded in DMF at room temperature. The monomer spectrum indicates one band centred at about 300 nm assignable to the π–π* transition biphenyl moiety in the structure. Poly(*O*-tolidine) spectrum is dominated by two broad ab-

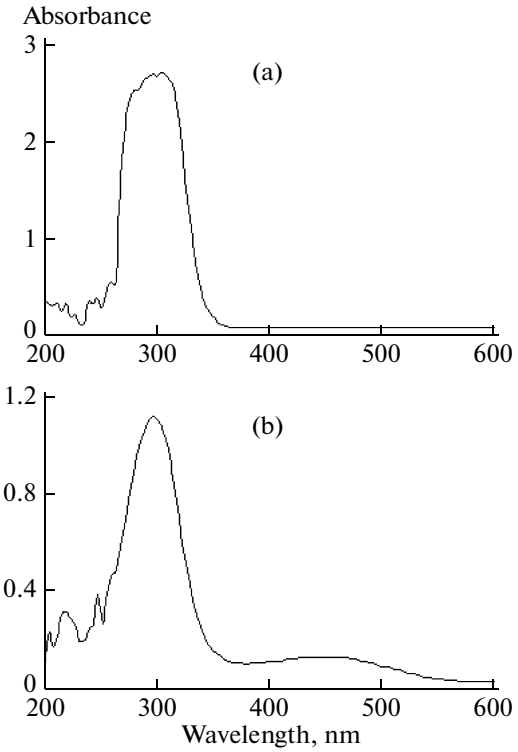

Fig. 8. UV-visible of: (a) 10^{-4} M of *O*-tolidine, (b) p-doped poly(*O*-tolidine).

sorption bands, at 300 nm (band 1) and 460 nm (band 2).

According to the general practice of band assignment, peak 1 is attributed to the $\pi-\pi^*$ transition of the biphenyl moieties in the poly(*O*-tolidine) structure or simply to the band gap of the polymer [21]. Band 2 is associated to the p-doped state of the polymer.

CONCLUSIONS

Electropolymerization of the *O*-tolidine was performed successfully in organic media containing a dry CH_2Cl_2 and 0.2 M Bu_4NBF_4. The cyclic voltammetry confirms clearly the formation of an electroactive poly(*O*-tolidine) with a positive doping and a reaction mechanism starting by coupling of two cation-radicals to form a dimmer. The electrochemical impedance spectroscopy (EIS) is a powerful tool providing a lot of information about the electrochemical characteristics of the subject being examined like double layer capacity, charge transfer resistance and solution resistance.

REFERENCES

1. A. F. Diaz and J. A. Logan, J. Electroanal. Chem. **111**, 111 (1980).
2. N. Oyama and Y. Ohnuki, Chem. Lett., 1759 (1983).
3. T. Kobayashi, H. Yoneyama, and H. Tamura, J. Electroanal. Chem. **161**, 419 (1984).
4. E. A. Kitani and J. Izumi, Bull. Chem. Soc. Japan **57**, 248 (1987).
5. K. Okabayashi, F. Goto, K. Abe, and T. Yoshida, Synth. Met. **18**, 365 (1987).
6. B. C. Sherman, W. B. Euler, and F. R. Ren, J. Chem. Educ. **71 (4)**, A94 (1994).
7. J. Yang, C. Zhao, D. Cui, J. Hou, M. Wan, and M. Xu, J. Appl. Polym. Sci. **56**, 831 (1995).
8. B. Sari and M. Talu, Synth. Met. **94**, 221 (1998).
9. Y. Huang, S. Xtao, and H. Tian, J. Funct. Polym. **11(3)**, 44 (1998).
10. G. J. Cruz, J. Morales, M. M. Castillo-Ortega, and R. Olayo, Synth. Met. **88**, 213 (1997).
11. S. Uemura, K. Teshima, S. Tokuda, N. Kobayashi, and R. Hirohashi, Synth. Met. **101**, 701 (1999).
12. E. M. Genies, A. Boyle, M. Lapkowski, and S. C. Tsintavis, Synth. Metal. **36**, 139 (1990).
13. X. G. Li, M. R. Huang, and W. Duan, Chem. Rev. **102**, 2925 (2002).
14. A. Buzarovska, I. Arsova, and Lj. Arsov, J. Serb. Chem. Soc. **66(1)**, 27 (2001).
15. F. D'Eramo, A. H. Arévalo, J. J. Silber, and L. Sereno, J. Braz. Chem. Soc. **5(3)**, 2213 (1998).
16. M. Naveen Kumar, M. Nagabhooshanam, M.Anand Rao, and M. Bhagvanth Rao, Cryst. Res. Technol. **36(3)**, 309 (2001).
17. C. P. Andrieux, P. Audebert, P. Hapiot, and J. M. Savéant; J. Phys. Commun. **95**, 10158 (1991).
18. M. S. Ureta-Zanartu, A. Alarcon, C. Berrios, G. I. Cardenas-Jiron, J. Zagal, and C. Gutierrez, J. Electroanal. Chem. **580**, 94 (2005).
19. R. K. Shervedani and S.A. Mozaffari, Surf. Coat. Technol. **198**, 123 (2005).
20. J. G. Killian, B. M. Coffey, F. Gao, T. O. Poehler, and P. C. Searson, J. Electrochem. Soc. **143**, 936 (1996).
21. J. Y. Lee and C. Q. Cui, J. Electroanal. Chem. **403**,109 (1996).